OMTM, Volume *18*

Supplemental Information

High-Resolution Histological Landscape of AAV DNA Distribution in Cellular Compartments and Tissues following Local and Systemic Injection

Junling Zhao, Yongping Yue, Aman Patel, Lakmini Wasala, Jacob F. Karp, Keqing Zhang, Dongsheng Duan, and Yi Lai

Title: High-resolution histological landscape of AAV DNA distribution in cellular compartments and tissues following intramuscular and intravenous injection

Authors: Junling Zhao[1], Yongping Yue[1], Aman Patel[2], Lakmini Wasala[1], Jacob F. Karp[1], Keqing Zhang[1], Dongsheng Duan[1,3,4,5,*], Yi Lai[1,*]

Address:

1. Department of Molecular Microbiology and Immunology, School of Medicine, University of Missouri, Columbia, Missouri, 65212, United States of America;

2. School of Medicine, Saint Louis University, St. Louis, Missouri, 63104, United States of America;

3. Department of Biomedical Sciences, College of Veterinary Medicine, University of Missouri, Columbia, Missouri, 65212, United States of America;

4. Department of Neurology, School of Medicine, University of Missouri, Columbia, Missouri, 65212, United States of America;

5. Department of Bioengineering, University of Missouri, Columbia, Missouri, 65212, United States of America.

Correspondence should be addressed to:

* Dongsheng Duan, Ph.D. or Yi Lai, Ph.D.

Department of Molecular Microbiology and Immunology,

Medical Sciences Building,

One Hospital Drive, Columbia, MO 65212, USA

Email: duand@health.missouri.edu or laiy@health.missouri.edu

Tel: 573-882-8989

Fax: 573-882-4287

Running title: *In situ* analysis of AAV DNA after local and systemic delivery

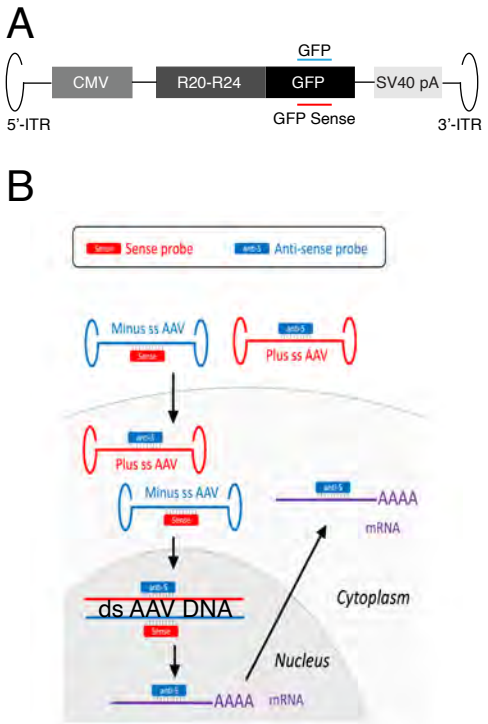

Supplemental Figure 1. AAV construct and the probe used in the study. A, A cartoon illustration of the construct used in this study. It contains the CMV.dystrophin R20-24.GFP expression cassette. The GFP probe binds to the sense strand of the GFP gene, while the GFP sense (GFP-S) probe labels the anti-sense strand of the GFP gene. **B,** the predicted targets that two GFP probes label. The GFP probe theoretically targets the plus single stranded (ss) AAV DNA, double stranded (ds) AAV DNA, and AAV RNA, while the GFP-S probe specifically labels the AAV DNA, including the minus ss AAV DNA and ds AAV DNA. ITR: inverted terminal repeat; R20-R24: dystrophin spectrin-like repeats 20-24; pA: SV40 polyadenylation signal.

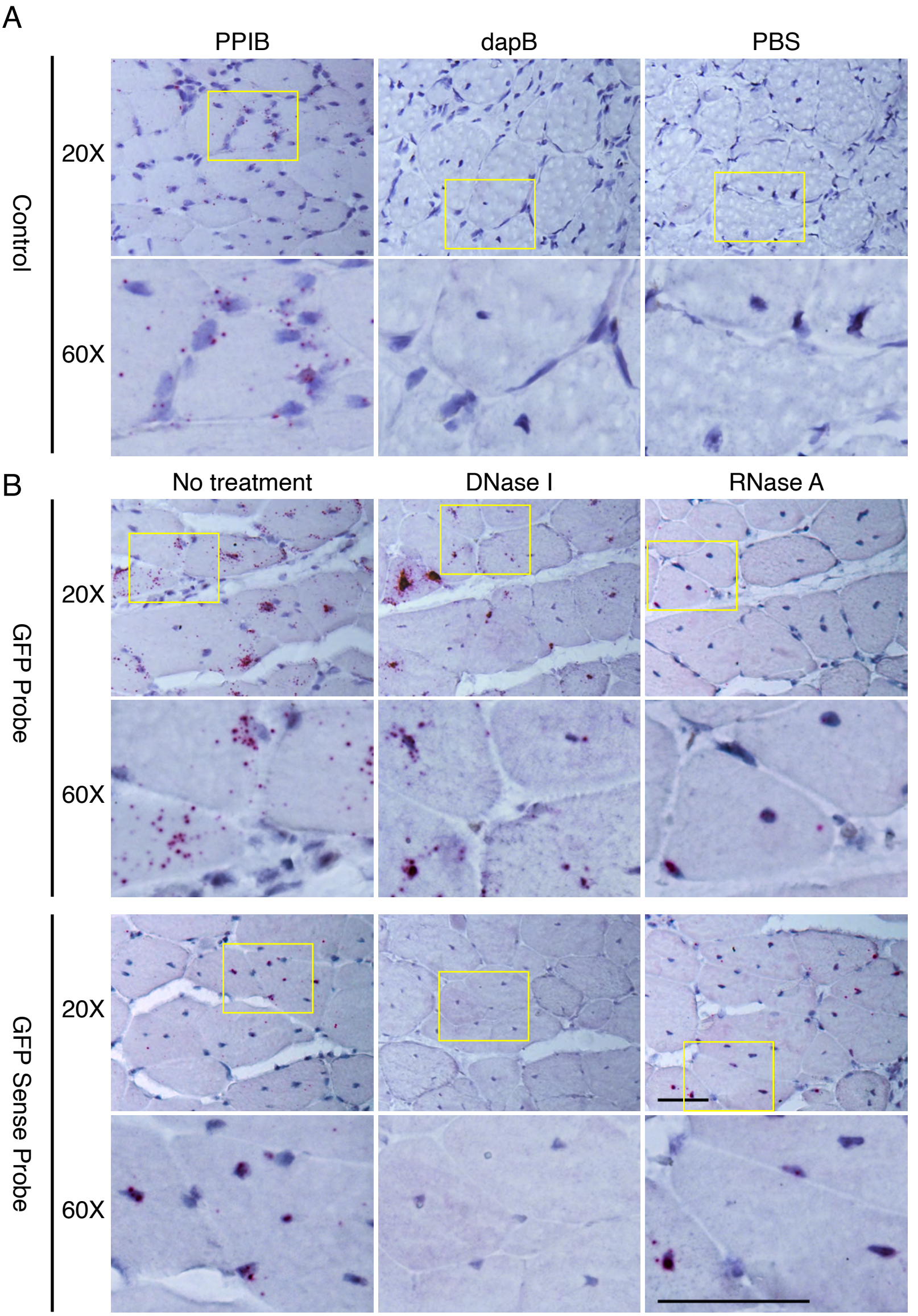

Supplemental Figure 2. Establishment of the specificity of RNAscope in detecting the AAV DNA and RNA in situ. A, The controls used in RNAscope. The positive probe labels the mRNA of the mouse peptidylprolyl isomerase B (PPIB) gene, a house keeping gene in mouse muscle. The negative probe recognizes the bacterial dapB mRNA. The PBS only is the no probe control. Strong signal was detected with the PPIB probe. No signal was detected with the dapB probe. The PBS control also showed no signal. **B,** Evaluation of the AAV DNA and RNA using the GFP probe and GFP-S probe in the tibialis anterior muscle that has received local injection of the AAV.R20-24.GFP vector. Four weeks after IM injection, without any pretreatment, hybridization with the GFP probe resulted in extensive cytoplasmic signals, which mostly reflected the AAV RNA distribution, while with the GFP-S probe hybridization, the signal was mainly confined to the nuclei of the muscle cells, which are the final destination of the AAV DNA. Following DNase pretreatment, compared with no pretreatment, the signals produced by the GFP probe were barely affected and still in the cytoplasm, confirming that the signals mostly arose from the AAV RNA. However, after DNase pretreatment, the GFP-S probe cannot detect any signal in the muscle section, confirming the specificity of the AAV DNA detection by the GFP-S probe. When pretreated with RNase before hybridization, the observed cytoplasmic signals by the GFP probe almost completely disappeared and a few signals were found in the nuclei, further confirming the specificity of detecting the AAV RNA by the GFP probe. As expected, RNase pretreatment did not change the distribution pattern of the signals detected by the GFP-S probe, further confirming the viral DNA specificity of the GFP-S probe. Scale bar: 20X-50 μm; 60x-50 μm.

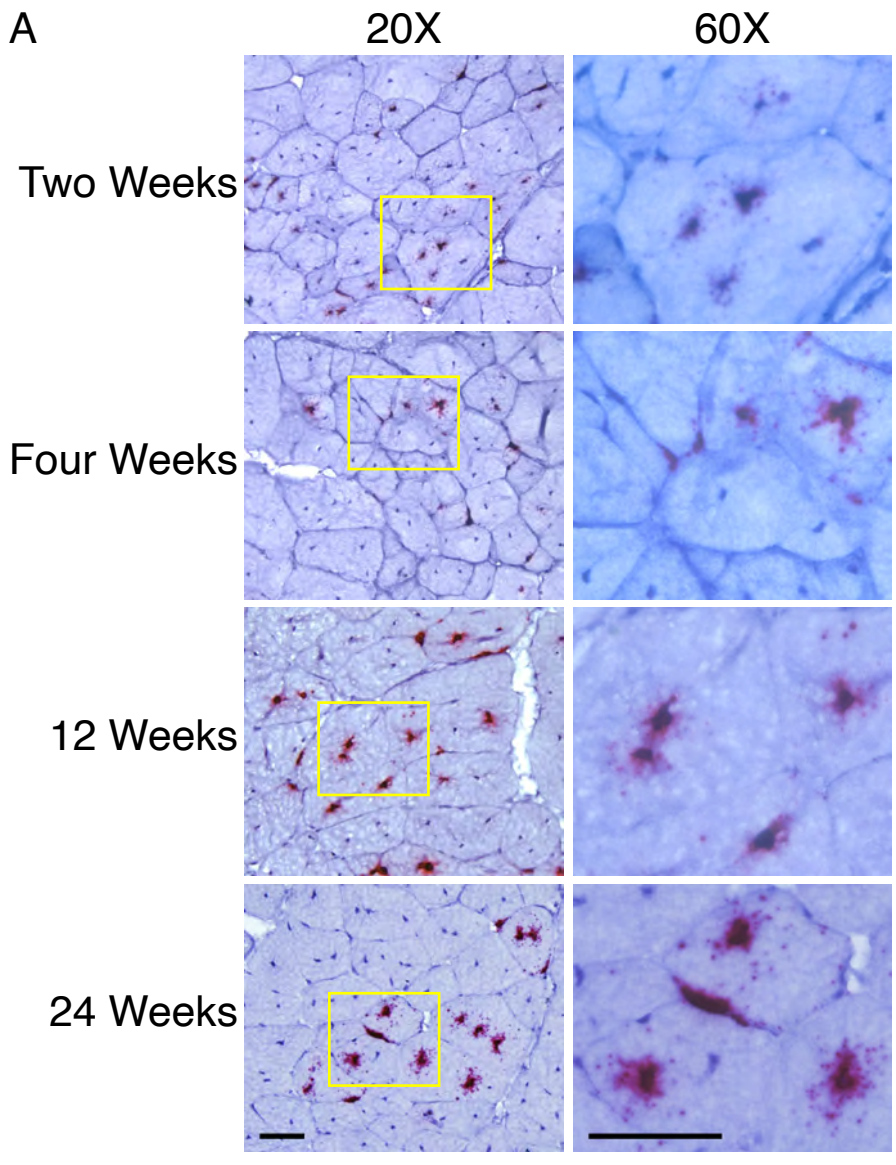

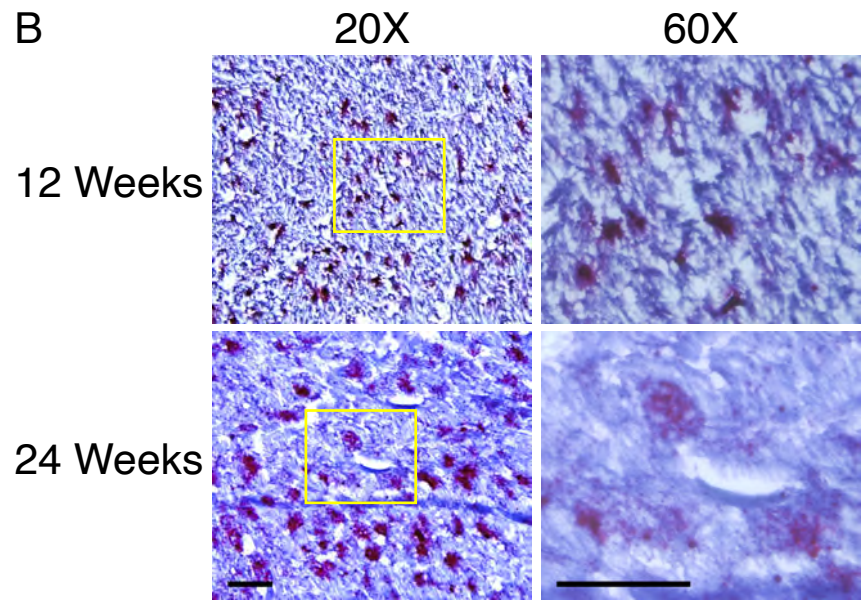

Supplemental Figure 3. Detection of the AAV RNA in the TA muscle and heart. **A,** detection of the AAV RNA with the GFP probe after DNase treatment in the TA muscle at two, four, 12 and 24 weeks after i.v. injection. **B,** detection of the AAV RNA with the GFP probe after DNase treatment in the heart at 12 and 24 weeks after i.v. injection. Scale bar: 20X-50 µm; 60x-50 µm.

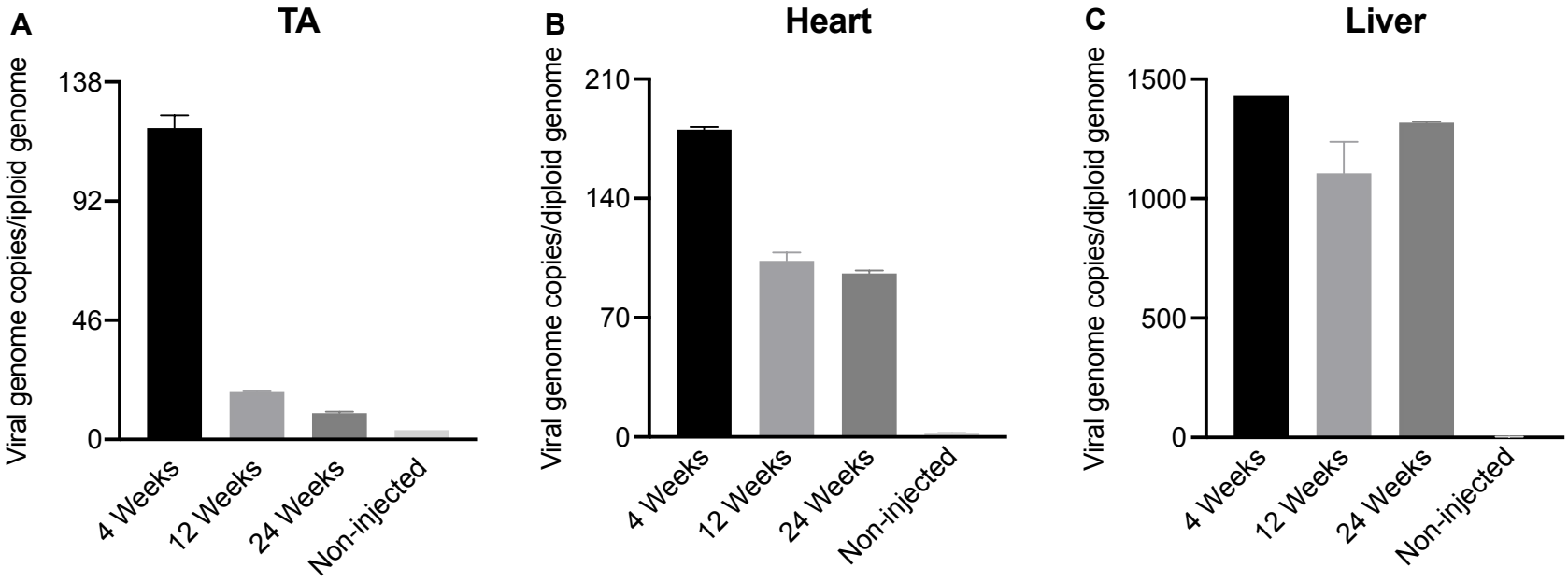

Supplemental Figure 4. Quantitative evaluation of the AAV genome copy number in the TA muscle, heart and liver after i.v. injection. The copy number of the AAV vector genome in the TA muscle, heart and liver was quantified by TaqMan PCR with the primers amplifying the SV40 polyA region. In the TA muscle (**A**), the viral genome copy number was reduced by ~10-folds between 4 weeks and 12 weeks after i.v. injection. But there was no substantial change between 12 weeks and 24 weeks after i.v. injection. In the heart (**B**), the copy number was reduced by ~2-folds between 4 weeks and 12 weeks after i.v. injection. But a similar copy number was observed between 12 weeks and 24 weeks after i.v. injection. In the liver (**C**), the copy number remained stable from 4 weeks to 24 weeks. n=2 for each group; Error bar: standard deviation (SD).

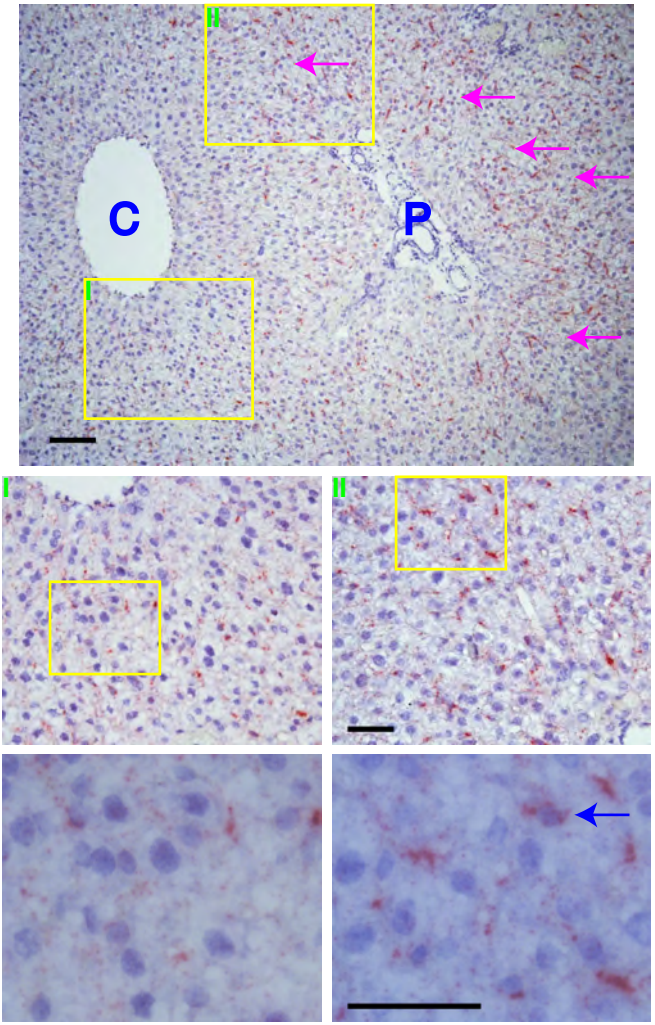

Supplemental Figure 5. AAV DNA distribution in the liver at 2 hrs after i.v. injection. At 2 hrs after i.v. injection, most of AAV DNA stayed outside the nuclei of hepatocytes, with individual nuclear localization (blue arrow). More AAV DNA (pink arrow) accumulated around the portal region (P) than the central vein region (C). Scale bar: 10x-100 μm; 20X-50 μm; 60x-50 μm.

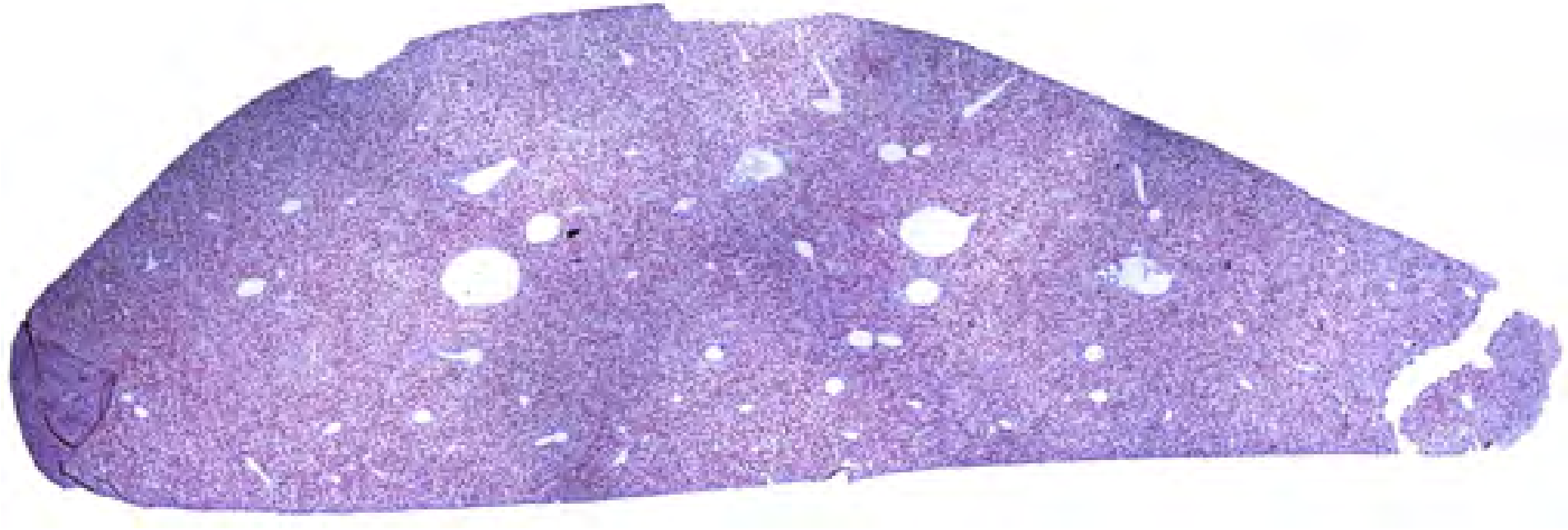

Supplemental Figure 6. Overview of the AAV DNA distribution in the left lobe of the liver. The AAV DNA was examined in the whole section of the left lobe of the liver at five days after i.v. injection. Even distribution of the AAV DNA was observed and almost all the hepato-cytes were transduced.

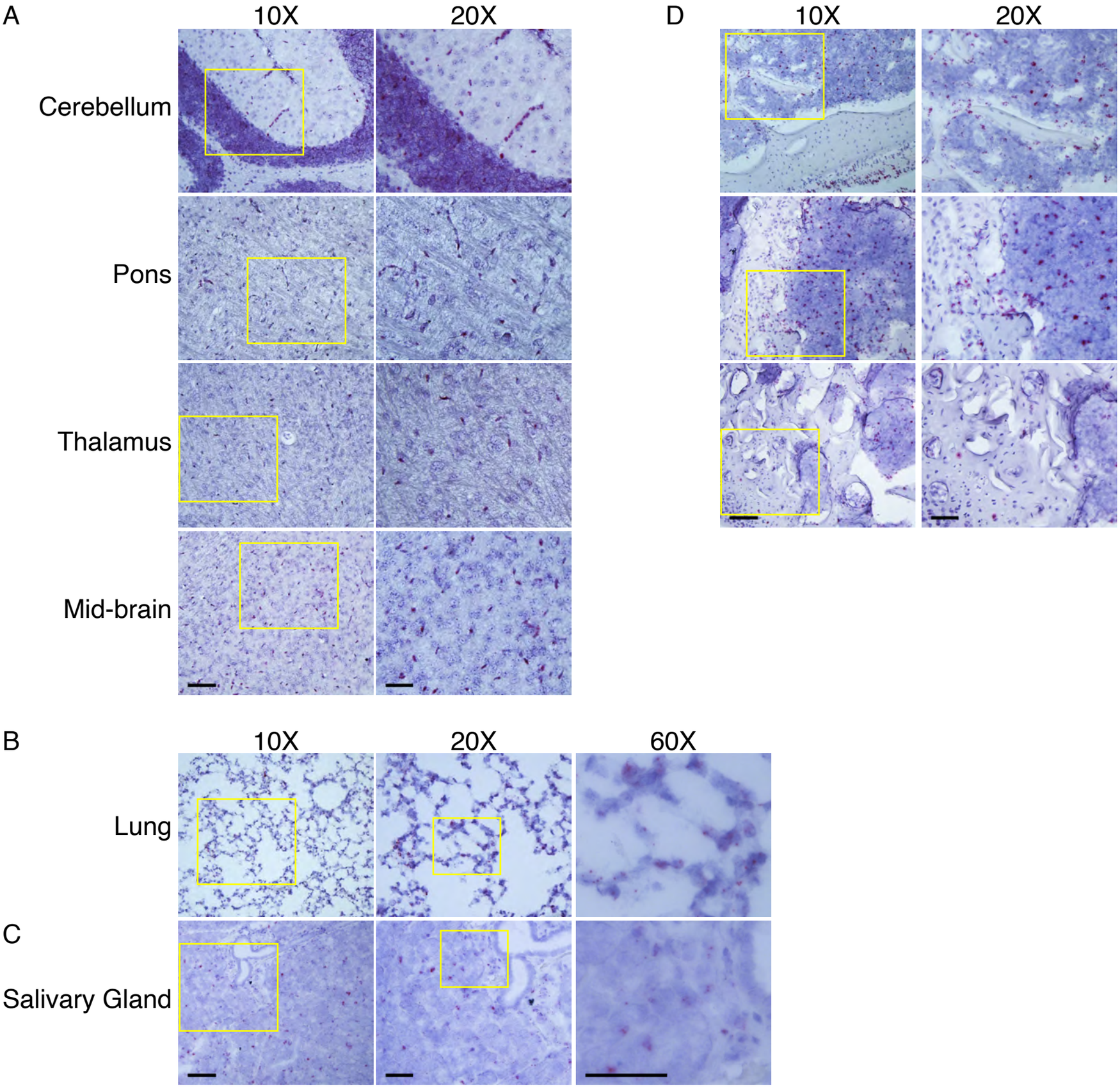

Supplemental Figure 7. AAV DNA distribution in the brain, bone marrow, lung and salivary glands at five days after i.v. injection. **A,** AAV DNA distribution in cerebellum, pons, thalamus and mid-brain. Relatively homogenous distribution was seen in the brain, with AAV DNA in endothelial cells, neurons, microglia and astrocytes. Scale bar: 10x-100 μm; 20X-50 μm. **B&C,** scattered AAV DNA distribution in the lung and submandibular salivary gland. The AAV DNA was seen in alveolar cells in the lung and acinar cells in the salivary glands. Scale bar: 10x-100 μm; 20X-50 μm; 60x-50 μm. **D,** distribution of the AAV DNA in the tibia bone marrow. Robust localization of the AAV DNA was seen in the tibia bone marrow, with a few positive signals in the cartilage bone. Scale bar: 10x-100 μm; 20X-50 μm.

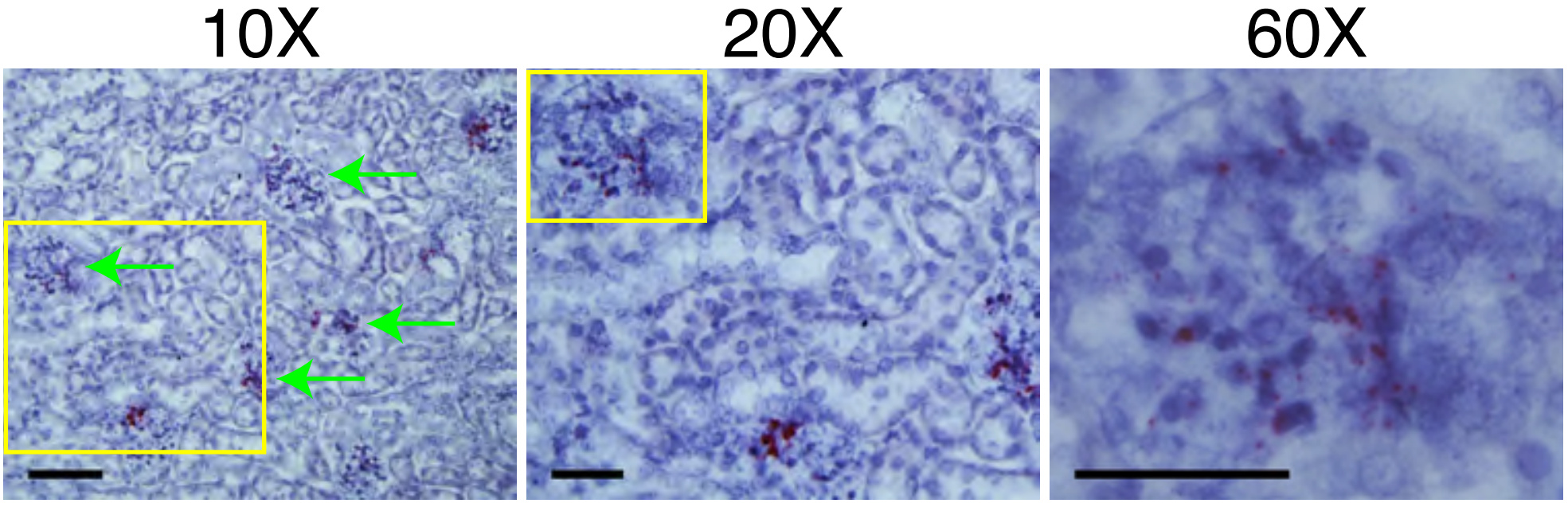

Supplemental Figure 8. AAV DNA in the kidney at 24 weeks after i.v. injection. The AAV DNA signal was dramatically reduced. The AAV DNA was mainly localized in the glomeruli (green arrow) and no AAV DNA was seen in the medulla. Scale bar: 10x-100 μm; 20X-50 μm; 60x-50 μm.

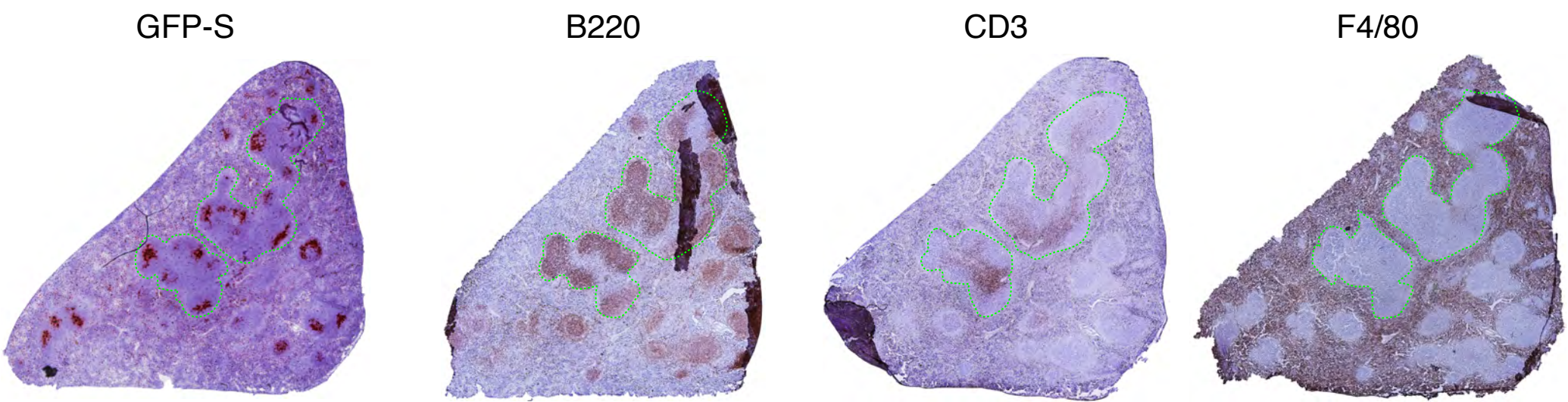

Supplemental Figure 9. Correlation of the AAV DNA with cell types in the spleen. Serial sections from the spleen harvested at five days after i.v. injection were labelled for the AAV DNA (GFP-S), B cells (B220), T cells (CD3) and macrophages (F4/80). The boundary of two representative follicles was marked with green dashed lines. The highly concentrated AAV DNA is co-localized with B-cell-dominant areas, while scattered cluster distribution of the AAV DNA is overlapped with macrophage-rich areas.

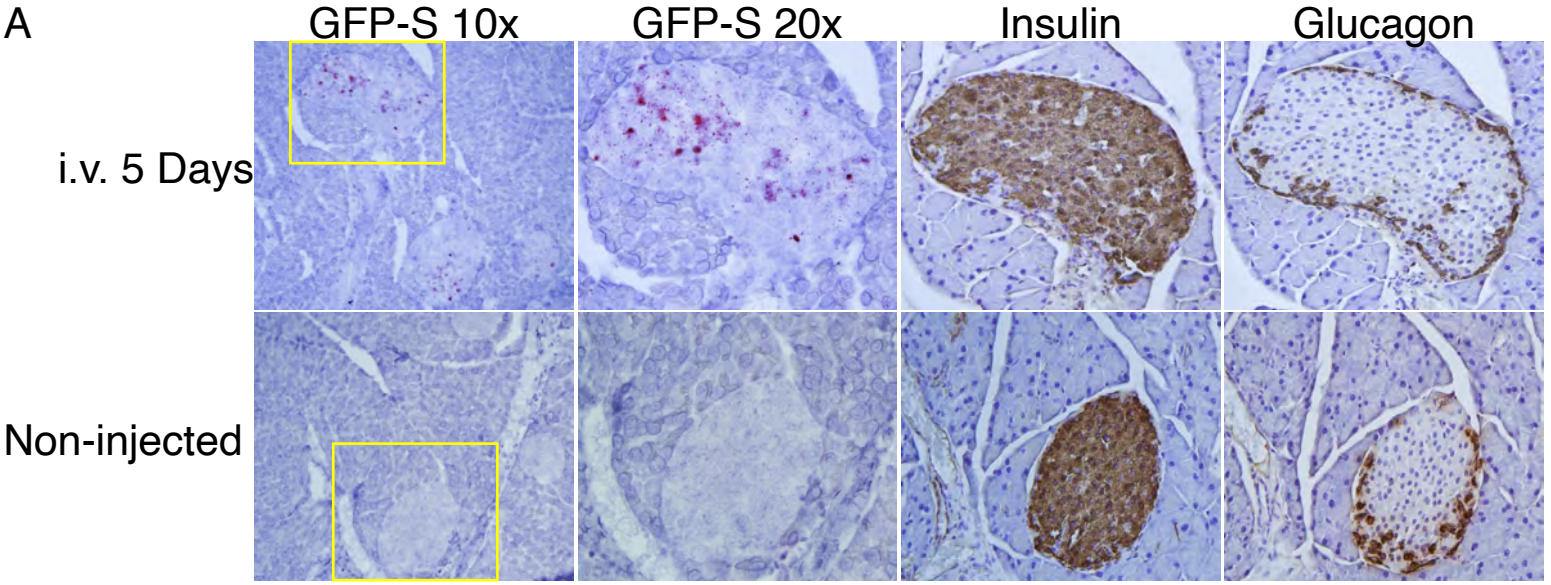

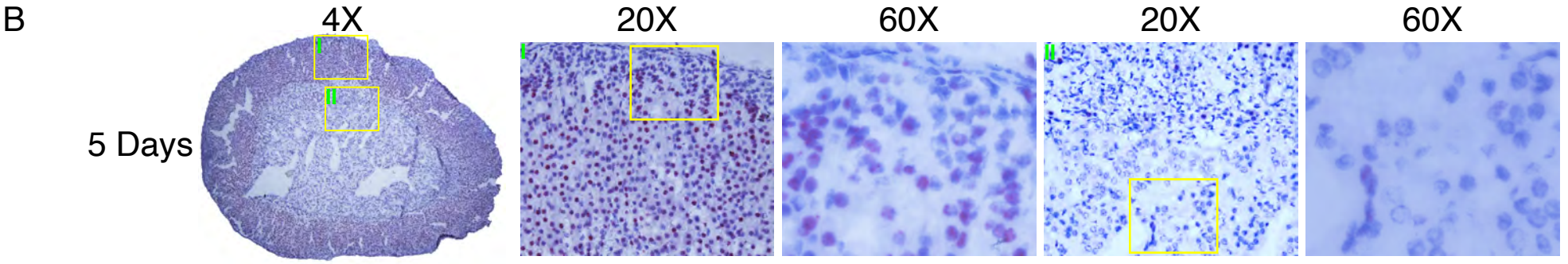

Supplemental Figure 10. AAV DNA distribution in the pancreas and adrenal glands at five days after i.v. injection. A, AAV DNA localization in the pancreas. The AAV DNA was predominantly localized in the islets of the pancreas. With insulin and glucagon IHC staining, the AAV DNA was mostly in the β cells of the islet. **B,** substantial amount of the AAV DNA was found in the cortex, especially in the zona fasciculata, with a few positive signals in the zona glomerulosa and the medulla.

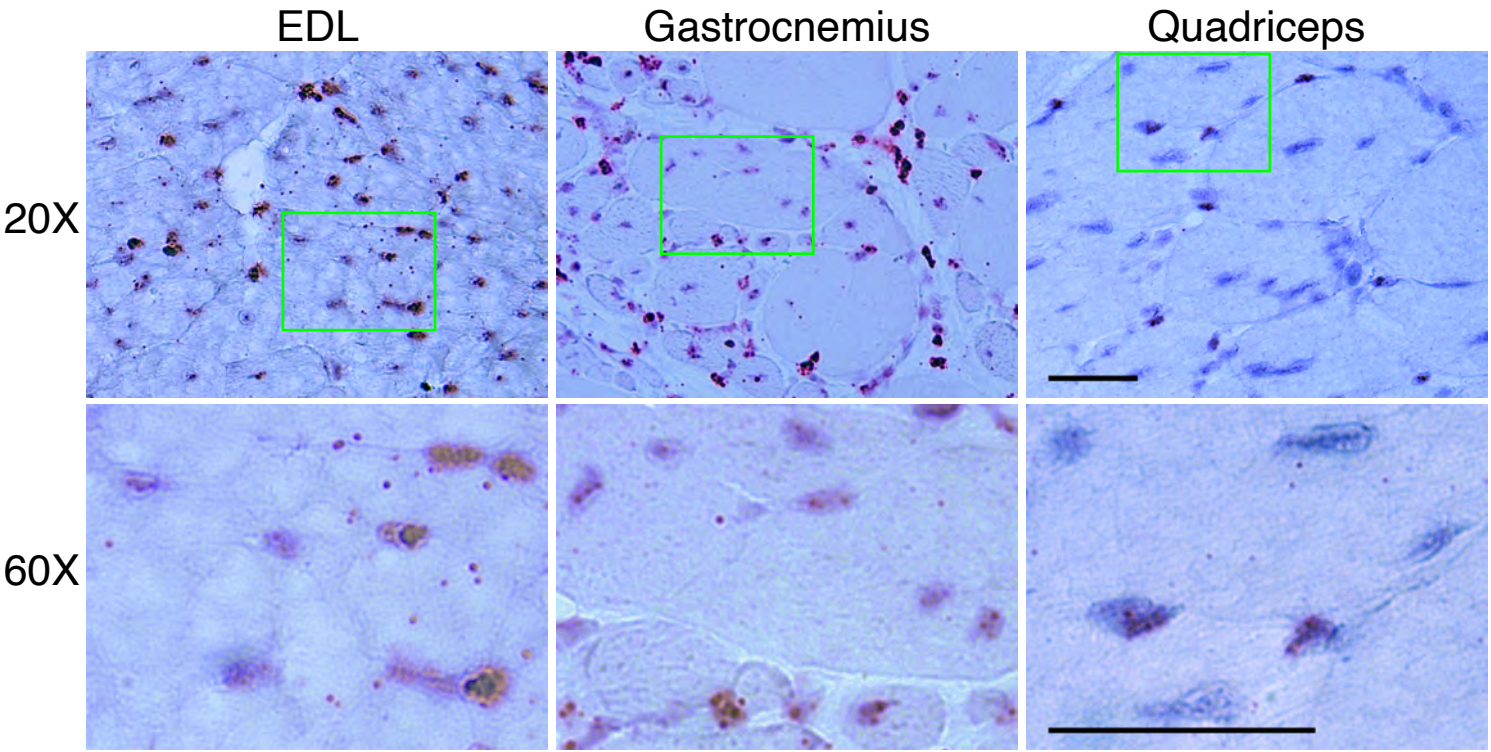

Supplemental Figure 11. Robust distribution of the AAV DNA in the neighboring muscles at five days after bilateral TA muscle injections. Significant distribution of the AAV DNA was seen in the EDL, gastrocnemius and quadriceps muscles, which are the neighboring muscles of the TA muscle. TA, tibialis anterior; EDL, extensor digitorum longus. Scale bar: 20X-50 μm; 60x-50 μm.

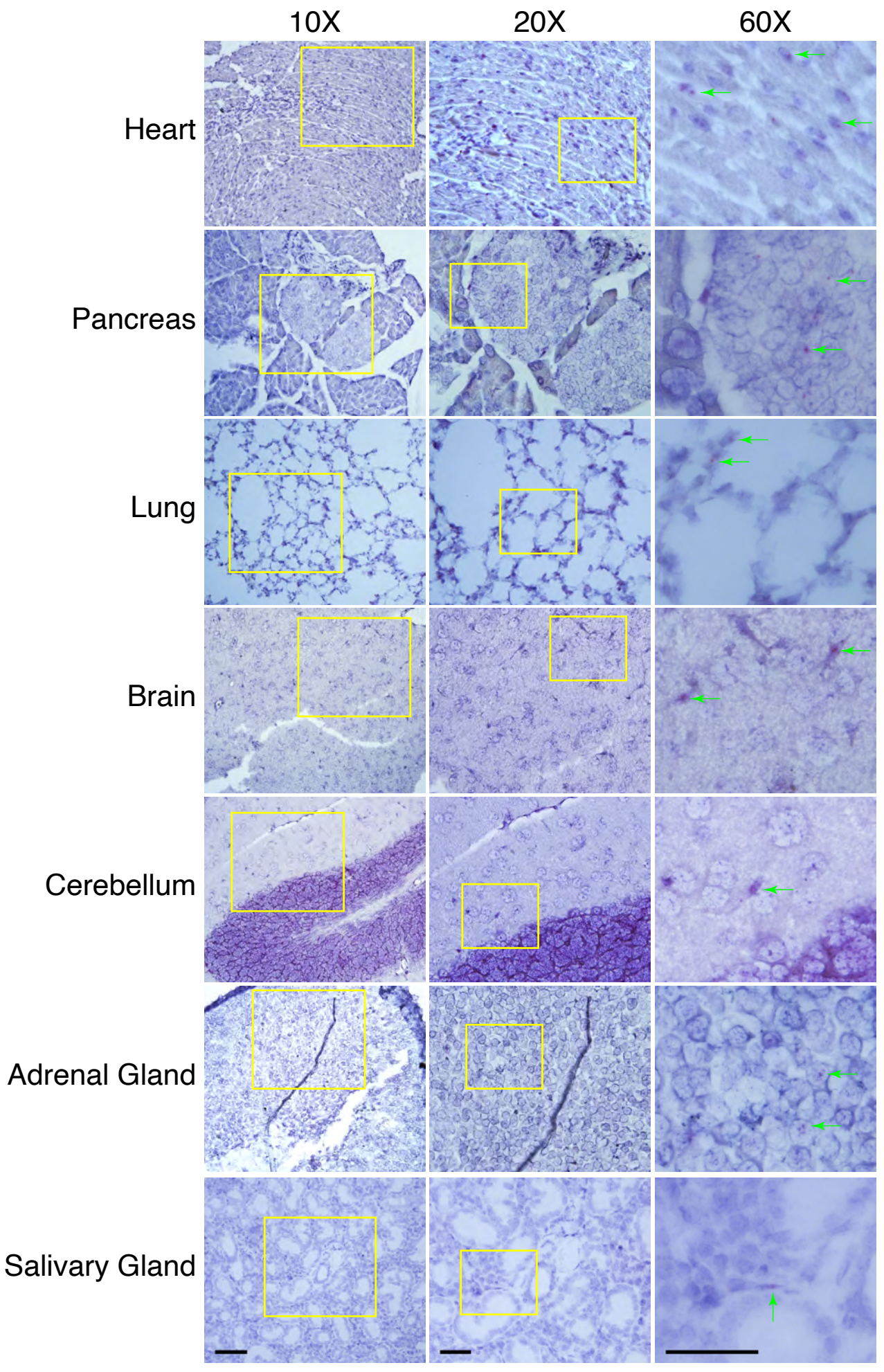

Supplemental Figure 12. Distribution of the AAV DNA in the heart, lung, brain, adrenal glands and salivary glands at five days after bilateral TA injections. i.m. injection leads to the distribution of the AAV DNA in multiple organs throughout the body. Spotty signals were observed in the heart, lung, brain, adrenal glands and submandibular salivary gland. Green arrow: AAV DNA. Scale bar: 10x-100 μm; 20X-50 μm; 60x-50 μm.